J|A|C|S
COMMUNICATIONS

Published on Web 10/05/2004

Glycosidic Torsional Motions in a Bicelle-associated Disaccharide from Residual Dipolar Couplings

Xiaobing Yi, André Venot, John Glushka, and James H. Prestegard*

Complex Carbohydrate Research Center, University of Georgia, Athens, Georgia 30602

Received July 17, 2004; Email: jpresteg@ccrc.uga.edu

The inherent flexibility of the oligosaccharides that decorate the surfaces of cells as parts of various glycolipids and glycoproteins has been recognized for some time.[1] The exact role that this flexibility might play in the function of these molecules is not clear, but at a minimum, a description of the conformational space sampled as motion occurs about various glycosidic bonds can provide insight into the possible structures that could be targets in various recognition events. It has, however, been difficult to obtain quantitative descriptions of motion in these molecules and, in particular, the amplitudes of motion as they occur over a wide range of time scales. There have been a number of spin relaxation studies that assign time scales to motion, but these often provide only a qualitative assessment of motional amplitudes.[2] Likewise, NOE-based structural studies have provided a qualitative indication of the presence of motion through incompatibilities with rigid models, but they seldom lead to more quantitative descriptions.[3] Here we apply residual dipolar couplings (RDCs) to the study of a particular disaccharide, *n*-butyl-4-*O*-*β*-D-galactopyranosyl-α-D-mannopyranoside (GMB). The analysis presented leads to a detailed description that is in excellent agreement with a molecular dynamics simulation of the motion and establishes a precedent for similar analyses of naturally occurring glycoconjugates.

Over the past few years, RDCs have emerged as very useful tools for elucidation of both structural and motional properties of biomolecules,[4] and several applications to oligosaccharides have appeared.[5] In general, structural information is available through an ability to determine the preferred alignment of various sugar rings in an oligosaccharide from the way in which the angle dependent dipolar coupling between various pairs of spin $^1/_2$ nuclei is averaged. This averaging is conveniently expressed in terms of factors derived from the average geometry of sugar rings and a set of order parameters[6]

$$\mathrm{RDC}_{ij} = \frac{D^{ij}_{\max}}{r^3_{ij}} \sum_{i,j=x,y,z} S_{ij} \cos\phi_i \cos\phi_j \qquad (1)$$

where the $D^{ij}_{\max}$ is a constant and the r_{ij} is the distance for a given pair of nuclei *i* and *j*, cos $\phi_{i(j)}$ are direction cosines for the interaction vector relative to an arbitrarily chosen fragment frame, and S_{ij} are order parameters describing the ordering of this frame relative to an alignment director. The order parameters can be determined by collecting a sufficient number of RDCs within the ring and solving a set of equations, in the form of eq 1, for these parameters. Diagonalizing the order matrix assembled from the order parameters yields a principal alignment frame that is common to all rings of a structure when they take their proper orientation in a composite structure.[6] Information about amplitudes of motion is, however, also available from the sizes of the elements in the diagonalized matrices. When the molecule is rigid, sizes of these elements will be identical for each ring. When internal motions exist, the sizes can be different. In principle, it is possible to interpret differences in terms of amplitudes of internal motions, but this can be difficult. Because interpretation of any differences in sizes of order tensor elements depends on knowing the orientation and size of a reference order tensor for the whole molecule, this tensor would have to be independently determined from additional RDC data collected on the molecule of interest.

In this work, we overcome the need for determination of an overall reference frame by anchoring one end of our disaccharide to a partially aligned bilayer medium using a short alkyl chain at the reducing end. This forces the reference frame to coincide with the frame determined for the reducing end sugar and eliminates the need for additional data. The highest level of alignment is also expected to be parallel to the alkyl chain and near the norm of the bilayer structures constituting the alignment medium. Using this strategy, internal motions can be described relative to the reducing end sugar, and better insight into the internal dynamics of this disaccharide can be obtained.

We first qualitatively examined the effect of the addition of the *n*-butyl chain to the disaccharide. This was done by collecting RDC data on the reducing disaccharide 4-*O*-*β*-D-galacto-pyranosyl-α-D-mannopyranose (GMOH, Sigma), on its α-methyl glycoside: methyl-4-*O*-*β*-D-galactopyranosyl-α-D-mannopyranoside (GMM) and on GMB, which were obtained by conventional syntheses described in the Supporting Information.[7] Samples for NMR were prepared at approximate 10 mM in a bilayerlike alignment medium formed from 2.0% (w/v) pentaethylene glycol monododecyl ether ($C_{12}E_5$, Sigma)/hexanol/water.[8] RDCs were subsequently measured on a Varian Inova spectrometer operating at 800 MHz for protons at 25 °C. An E.COSY style $^{13}C-^1H$ HSQC experiment that allowed the measurement of both one-bond $^{13}C-^1H$ couplings and longer range $^1H-^1H$ homonuclear couplings provided the majority of the data.[9] The measured RDCs are summarized in Table 1, and additional experimental details are supplied as Supporting Information.

The resulting RDC data in Table 1 show that there are significant changes in the measured RDCs on increasing alkyl chain length from methyl to *n*-butyl. Adding a methyl group to the reducing end of GMOH changes values of dipolar couplings only slightly. However, the fact that changes are not uniform indicates a significant reorientation. The fact that the derived orientation for the methyl analogue GMM does not agree with alignment predicted from sterically induced alignment models (PALES[11]) suggests that even this small addition of a hydrophobic group is inducing some specific association with the medium.[12] The change on adding an *n*-butyl chain is more dramatic. The RDC of $^{13}C_4-^1H_4$ on the galactopyranosyl ring in GMB reaches a very large value of 96 Hz. On comparing one-bond $^{13}C-^1H$ RDCs to the corresponding couplings for GMOH and GMM, the signs of many couplings have changed and the sizes of some couplings have increased by an order of magnitude or more, indicating the disaccharide has been

10.1021/ja045697t CCC: $27.50

Table 1. RDCs for GMOH, GMM and GMB in 2.0% $C_{12}E_5$/ Hexano/Water Medium at 25 °C

		RDCs (Hz)		
		GMOH[a,b]	GMM[b]	GMB[c]
Gal	C_1H_1	3.0	1.6	−24.8
	C_2H_2	2.2	2.0	−11.5
	C_3H_3	3.2	1.7	−17.3
	C_4H_4	0.2	1.9	95.6
	C_5H_5	1.1	0.7	−23.7
	H_1H_2			−8.4
	H_1H_3			10.0
	H_2H_3			7.3
	H_2H_4			−3.6
	H_3H_4			−0.8
Man	C_1H_1	−3.3	−3.2	−36.9
	C_2H_2	1.3	1.5	−3.8
	C_3H_3	6.1	2.1	18.9
	C_4H_4	6.4	2.3	35.0
	C_5H_5	0.9	2.6	13.1
	H_3H_4			4.5
	H_3H_5			−21.1
	H_4H_5			8.6

[a] The sample is a mixture of α and β conformers and the data shown here is from α conformer. [b] The data were obtained from the constant time coupling enhanced HSQC experiment.[5a] The measurement of $^{13}C-^{13}H$ couplings were done by projecting the peaks along the F_1 dimension. After inverse transformation and zero filling of the resulting 1D spectra, couplings were measured by peak picking and followed by nonlinear peak simulation using the program NMRPipe.[10] [c] The line width is broad and the $^1H-^1H$ couplings for GMB were extracted using a center of mass peak picking method.

immobilized and reoriented by the *n*-butyl alkyl chain. The data are suggestive of a model in which increasing the alkyl chain length changes the mechanism of alignment from a collisional one to one in which alkyl chain insertion into the bilayer systems reorients the oligosaccharide.[12] Reorientation by *n*-butyl chain insertion should selectively immobilize the alkylated ring, making the first ring a suitable reference for analysis of internal motion.

A quantitative analysis of the GMB data proceeded using the general methods described in the introductory paragraphs. The individual galactopyranosyl (Gal) and mannopyranoside (Man) rings were modeled as rigid segments. The coordinates for these rings were generated and the energies were minimized using AMBER 7.0 and the GLYCAM_04 force field.[13] To validate the rigidity of Gal and Man, average RDCs from molecular dynamics (MD) trajectory snapshots were back-calculated using eq 1, where the best order tensor described below was selected and the alignments were obtained by RMS fitting of the heavy atoms on pyranose rings. The data supported the use of a rigid pyranose structure in that the RDCs back-calculated using the derived order matrix for each ring and averaging over points in the trajectory reproduced couplings with a linear correlation coefficient of 0.99 and with a standard deviation of 4.2 Hz, as shown in Figure 3b. Order tensor analysis[6] of the RDCs for GMB in 2.0% $C_{12}E_5$/ hexanol/water was performed for each ring using the program REDCAT.[14] The resulting alignment tensor axis directions for each individual pyranose ring and the histograms of the largest order parameter in magnitude, S_{zz}, are shown in Figure 1. The S_{zz} is clearly negative for the Gal residue. Negative S_{zz} values are consistent with ordering along the bilayer normal, which is perpendicular to the magnetic field in this alignment medium. The alternation between positive and negative S_{zz} values seen in Figure 1d for residue Man is indicative of a large departure from simple axially symmetric order. However, it remains significant that the axis consistent with the large negative S_{zz} value lies nearly parallel to the $C_1-O_1-C_{1(butyl)}$ vector that would represent the beginning of the *n*-butyl chain. This supports the suggested mechanism of anchoring.

The average structure can be assembled by rotation of the rings to superpose the principal order tensor frames. The best solutions

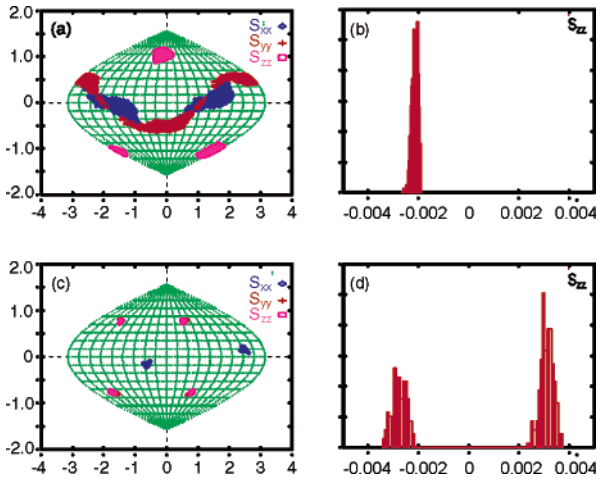

Figure 1. Sauson−Flamsteed projections of resulting alignment tensor axis directions in an arbitrary molecular frame and the histograms of S_{zz} for Gal (a and b) and of Man (c and d) in GMB. In the order tensor analysis, errors were adjusted to 8 Hz, which is about 10% of the experimental RDCs' range.

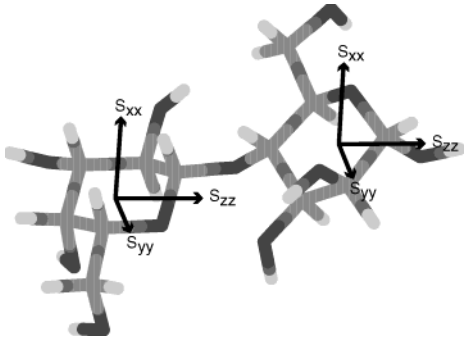

Figure 2. Average NMR structure for GMB obtained by superposition of the principal order tensor frames for Gal and Man residues.

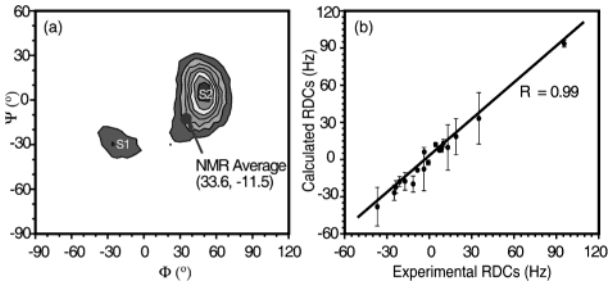

Figure 3. MD simulation results for GMM in water at 300 K for 20 ns. (a) Contour plot of the Φ and Ψ distribution. (b) Correlation between experiment RDCs and calculated average RDCs from the MD trajectory. The details are supplied as Supporting Information.

in an RMSD sense were picked for each ring to assemble the average structure. Because of the orientational degeneracy of RDCs[4b] there will be four possible ways to assemble the two fragments. On the basis of the facts that the glycosidic bond angle should be around 117° and strong NOEs between Gal-H_1 and Man-H_4 are observed, three orientations can be excluded. The resulting average NMR structure shown in Figure 2 gives a bond angle of 116° and Φ, Ψ torsion angles of +33.6 and −11.5° respectively (Φ and Ψ are defined as $H_1-C_1-O_4-C_4$ and $C_1-O_4-C_4-H_4$). These angles agree reasonably well with those from an X-ray structure of 4-*O*-β-D-galactopyranosyl-a−D-mannopyranose ethanol solvate dehydrate (117.0, 28.0, and 10.4°).[15]

It is significant that the principal order parameters for the two fragments are different. As shown in Figure 1, the best principal

S_{xx}, S_{yy}, and S_{zz} values are 6.95×10^{-4}, 1.38×10^{-3}, and -2.08×10^{-3} for the Gal residue and 8.55×10^{-5}, 2.92×10^{-3}, and -3.01×10^{-3} for the Man residue. If the two fragments were rigidly connected, their order parameters should be equivalent. The reduction in the general degree of order (GDO) [6] by approximately 38% for Gal is indicative of significant internal motion between rigid Gal and Man residues. If this motion were to be approximated by uniform wobbling in a cone of half angle θ, it could be described by eq 2, and θ estimated at 40°.

$$\frac{\int_0^\theta \frac{3\cos^2\theta - 1}{2}\sin\theta \, d\theta}{\int_0^\theta \sin\theta \, d\theta} = 0.62 \qquad (2)$$

The motion is obviously a little more complex since S_{xx}, S_{yy}, and S_{zz} are not reduced equally, as they would be in a cone motion. S_{zz} is reduced by about 30% while the S_{xx} and S_{yy} change more substantially, moving toward values consistent with averaging of the values seen for the mannose ring. This suggests that the dominant motions are rotations about the *z* axis, motions that can average components along the *x* and y axes. In the structure shown in Figure 2, the *z* axis lies approximately along the glycosidic linkage, indicating some correlated motion about Φ and Ψ to be responsible for the reduction of order parameters.

MD simulations can give a more detailed picture of possible motions about the glycosidic bond. It is also of considerable interest to evaluate the ability of these simulations to properly predict motional amplitudes. A 20 ns MD simulation of GMM in explicit water was, therefore, carried out at 300 K under periodic boundary conditions using AMBER 7.0 with the GLYCAM_04 force field on Linux cluster. The simulation was performed at 300 K with an integration time step of 1 fs and with snapshots stored every 500 fs. The Φ and Ψ distribution from the snapshots was plotted in Figure 3a. It is clear from Figure 3a that the GMM is moving back and forth between two states with (Φ, Ψ) angles of (−25, −30°) for state 1 (S1) and (+50, +5°) for state 2 (S2). The populations from the MD simulation for S1 and S2 are 17% and 83% respectively.

It is possible to model the RDC data on GMB to include averaging between two states using the program REDCAT.[14] The measured RDC data is an average contributed from all possible states. To improve the accuracy of this modeling, the MD geometries of S1 and S2 were first submitted to a full geometry optimization using the program Gaussian 98.[16] The optimizations were carried out using the Onsager reaction field model in aqueous solution with a B3LYP hybrid density functional model and with a 6-31G(d) basis set, giving the (Φ, Ψ) of (−37.7, −27.4°) for S1 and (+47.7, −6.7°) for S2. Under the assumption that the immobilized rigid Man ring could be used as a reference segment, the coordinates of the two states were translated and rotated by RMS fitting of the heavy atoms of the Man ring and the coordinates entered into REDCAT duplicating entries to simulate relative populations. In this way the population of S1 was increased from 0% to 100% with a step size of 10%. Only the ratios of 1:9 (10%), 1:4 (20%), and 3:7 (30%) gave acceptable solutions. The RMSDs between the calculated RDCs and experimental observations are 1.23, 1.22, and 4.06 Hz for these ratios. Since both S1:S2 = 1:9 and S1:S2 = 1:4 give equally good predictions, we conclude that the conformational populations are 15% ± 10% for S1 and 85 ± 10% for S2. The results from direct analysis of the NMR data and the MD trajectories are, thus, in excellent agreement.

In conclusion, we have demonstrated that the orientation of molecules in partially aligned bilayer media can be controlled by introducing an alkyl chain of appropriate length to a molecule of interest, and that, for flexible molecules, the molecular fragment most immobilized becomes an appropriate reference for the evaluation of internal motion. The differences between the order tensors determined from RDCs for connected segments can then be used to quantitate the level of internal motion. This has been demonstrated here for motions about the glycosidic bond in the simple disaccharide, GMB. However, the methodology is readily extended to more complex oligosaccharides from glycolipids where alkyl anchors can model natural lipid chains[17] and to more complex oligosaccharides from glycoproteins where immobilization of the protein component can serve to define a reference segment.

Acknowledgment. This work is supported by NIH Grants GM33225 and RR05351. We would like to thank Dr. R. J. Woods, W. S. York, and Dr. H. Valafar for helpful discussions.

Supporting Information Available: Text giving experimental procedures to synthesize GMM and GMB, a figure showing NMR spectra for GMB in D_2O and in $C_{12}E_5$/hexanol/water medium, and tables of back-calculated RDCs from MD trajectories and back-calculated RDCs using REDCAT averaging. This material is available free of charge via the Internet at http://pubs.acs.org.

References

(1) (a) Dwek, R. A. *Biochem. Soc. Trans.* **1995**, *23*, 1−25. (b) Poveda, A.; Jiménez-Barbero, J. *Chem. Soc. Rev.* **1998**, *27*, 133−143.
(2) (a) Daragan, V. A.; Mayo, K. H. *Prog. Nucl. Magn. Reson. Spectrosc.* **1997**, *31*, 63−105. (b) Frueh, D. *Prog. Nucl. Magn. Reson. Spectrosc.* **2002**, *41*, 305−324.
(3) Schleucher, J.; Wijmenga, S. S. *J. Am. Chem. Soc.* **2002**, *124*, 5881−5889.
(4) (a) Tjandra, N.; Bax, A. *Science* **1997**, *278*, 1111−1113. (b) Prestegard, J. H.; Al-Hashimi, H. M.; Tolman, J. R. *Q. Rev. Biophys.* **2000**, *33*, 371−424. (c) Tolman, J. R. *Curr. Opin. Struct. Biol.* **2001**, *11*, 523−539. (d) Bax, A. *Protein Sci.* **2003**, *12*, 1−16.
(5) (a) Tian, F.; Al-Hashimi, H. M.; Craighead, J. L.; Prestegard, J. H. *J. Am. Chem. Soc.* **2001**, *123*, 485−492. (b) Martin-Pastor, M.; Bush, C. A. *Carbohyd. Res.* **2000**, *323*, 147−155. (c) Lycknert, K.; Maliniak, A.; Widmalm, G. *J. Phys. Chem.* **2001**, *A 105*, 5119−5122.
(6) Losonczi, J. A.; Andrec, M.; Fischer, M. W. F.; Prestegard, J. H. *J. Magn. Reson.* **1999**, *138*, 334−342.
(7) Schimdt, R. R.; Kinzy, W. *Ad. Carbohydr. Chem. Biochem.* **1994**, *50*, 21−123.
(8) (a) Jonstromer, M.; Strey, R. *J. Phys. Chem.* **1992**, *96*, 5993−6000. (b) Salamat, G.; Kaler, E. W. *Langmuir* **1999**, *15*, 5414−5421.
(9) Willker, W.; Leibfritz, D. *J. Magn. Reson.* **1992**, *99*, 421−425.
(10) Delaglio, F.; Grzesiek, S.; Vuister, G. W.; Zhu, G.; Pfeifer, J.; Bax, A. *J. Biomol. NMR.* **1995**, *6*, 277−293.
(11) Zweckstetter, M.; Bax, A. *J. Am. Chem. Soc.* **2000**, *122*, 3791−3792.
(12) Yi, X. B.; Prestegard, J. H. Manuscript in preparation.
(13) Case, D. A.; Pearlman, D. A.; Caldwell, J. W.; Cheatham, T. E., III; Wang, J.; Ross, W. S.; Simmerling, C. L.; Darden, T. A.; Merz, K. M.; Stanton, R. V.; Cheng, A. L.; Vincent, J. J.; Crowley, M.; Tsui, V.; Gohlke, H.; Radmer, R. J.; Duan, Y.; Pitera, J.; Massova, I.; Seibel, G. L.; Singh, U. C.; Weiner, P. K.; Kollman, P. A. *AMBER Revision 7.0*, University of California, San Francisco, 2002. (b) Woods, R. J. *GLYCAM_04*, http://glycam.ccrc.uga. edu /index.html.
(14) Valafar, H.; Prestegard, J. H. *J. Magn. Reson.* **2004**, *167*, 228−241.
(15) Burden, C.; Mackie, W.; Sheldrick. *Acta Crystallogr. C*, **1986**, *42*, 177−179.
(16) Frisch, M. J.; Trucks, G. W.; Schlegel, H. B.; Scuseria, G. E.; Robb, M. A.; Cheeseman, J. R.; Zakrzewski, V. G.; Montgomery, J. A.; Stratmann, R. E.; Burant, J. C.; Dapprich, S.; Millam, J. M.; Daniels, A. D.; Kudin, K. N.; Strain, M. C.; Farkas, O.; Tomasi, J.; Barone, V.; Cossi, M.; Cammi, R.; Mennucci, B.; Pomelli, C.; Adamo, C.;, Clifford, S.; Ochterski, J.; Petersson, G. A.; Ayala, P. Y.; Cui, Q.; Morokuma, K.; Malick, D. K.; Rabuck, A. D.; Raghavachari, K.; Foresman, J. B.; Cioslowski, J.; Ortiz, J. V.; Stefanov, B. B.; Liu, G.; Liashenko, A.; Piskorz, P.; Komaromi, I.; Gomperts, R.; Martin, R. L.; Fox, D. J.; Keith, T.; Al-Laham, M. A.; Peng, C. Y.; Nanayakkara, A.; Gonzalez, C.; Challacombe, M.; Gill, P. M. W.; Johnson, B. G.; Chen, W.; Wong, M. W.; Andres, J. L.; Head-Gordon, M.; Replogle, E. S.; Pople, J. A. *Gaussian 98 Revision A.11.3*, Gaussian, Inc.: Pittsburgh, PA, 1998.
(17) Hare, B. J.; Howard, K. P.; Prestegard, J. H. *Biophys. J.* **1993**, *64*, 392−398.

JA045697T